BJR
© 2016 The Authors. Published by the British Institute of Radiology

Received: 8 December 2015 | Revised: 9 August 2016 | Accepted: 12 September 2016

http://dx.doi.org/10.1259/bjr.20151033

Cite this article as:
Koob M, Rousseau F, Laugel V, Meyer N, Armspach J-P, Girard N, et al. Cockayne syndrome: a diffusion tensor imaging and volumetric study. *Br J Radiol* 2016; **89**: 20151033.

FULL PAPER

Cockayne syndrome: a diffusion tensor imaging and volumetric study

[1,2]MÉRIAM KOOB, MD, PhD, [2,3]FRANÇOIS ROUSSEAU, PhD, [4]VINCENT LAUGEL, MD, PhD, [5]NICOLAS MEYER, MD, PhD, [2]JEAN-PAUL ARMSPACH, PhD, [6]NADINE GIRARD, MD, PhD and [2,7]JEAN-LOUIS DIETEMANN, MD, PhD

[1]Service de Radiopédiatrie/Imagerie 2, CHU de Strasbourg, Hôpital de Hautepierre, Strasbourg, France
[2]Laboratoire ICube, UMR 7357/FMTS/Université de Strasbourg-CNRS, Strasbourg, France
[3]Institut Mines-Telecom, Telecom Bretagne, INSERM, LATIM UMR, Brest, France
[4]Service de Neurologie Pédiatrique, Hôpital de Hautepierre, Strasbourg, France
[5]Département de santé publique, d'Informatique médicale et de biostatistiques, CHU de Strasbourg, Hôpital civil, Strasbourg, France
[6]Service de Neuroradiologie Diagnostique et Interventionnelle, APHM Timone, Aix Marseille Université, CRMBM, UMR CNRS, Marseille, France
[7]Service de Neuroradiologie/Imagerie 2, CHU de Strasbourg, Hôpital de Hautepierre, Strasbourg, France

Address correspondence to: Dr Mériam Koob
E-mail: *meriam.koob@chru-strasbourg.fr*

Objective: Cockayne syndrome (CS) is a rare disorder characterized by severe brain atrophy, white matter (WM) hypomyelination and basal ganglia calcifications. This study aimed to quantify atrophy and WM abnormalities using diffusion tensor imaging (DTI) and volumetric analysis, to evaluate possible differences between CS subtypes and to determine whether DTI findings may correspond to a hypomyelinating disorder.
Methods: 14 patients with CS and 14 controls underwent brain MRI including DTI and a volumetric three-dimensional T_1 weighted sequence. DTI analysis was made through regions of interest within the whole brain to obtain fractional anisotropy (FA) and apparent diffusion coefficient (ADC) values and in the left centrum semiovale to obtain DTI eigenvalues. The Student's *t*-test was used to compare patients and controls, and CS subtypes. Given the small number of patients with CS, they were pooled into two groups: moderate (CS1/CS3) and severe (CS2/cerebro-oculo-facio-skeletal syndrome).
Results: Total brain volume in CS was reduced by 57%, predominantly in the infratentorial area (68%) ($p < 0.001$). Total brain volume reduction was greater in the severe group, but there was no difference in the degree of infratentorial atrophy in the two groups ($p = 0.7$). Mean FA values were lower, whereas ADC was higher in most of the WM in patients with CS ($p < 0.05$). ADC in the splenium of the corpus callosum and the posterior limb of the internal capsule and FA in the cerebral peduncles were significantly different between the two groups ($p < 0.05$). Mean ADC values corresponded to a hypomyelinating disorder. All DTI eigenvalues were higher in patients with CS, mainly for transverse diffusivity (+51%) ($p < 0.001$).
Conclusion: DTI and volumetric analysis provide quantitative information for the characterization of CS and may be particularly useful for evaluating therapeutic intervention.
Advances in knowledge: DTI combined with volumetric analysis provides additional information useful for not only the characterization of CS and distinction of clinical subtypes but also monitoring of therapeutic interventions.

INTRODUCTION

Cockayne syndrome (CS) is a very rare autosomal recessive multisystem disorder belonging to the family of DNA repair diseases. Clinical features include progressive neurologic and sensory impairment, photosensitivity, cachectic dwarfism and a typical facial appearance. The disease is considered to be very likely if the major clinical criteria (growth failure, mental retardation) and at least three of the minor clinical criteria (photosensitivity, pigmentary retinopathy or cataract, deafness, dental caries, cachectic dwarfism) are present. The diagnosis is confirmed by biochemical (inhibition of RNA synthesis after ultraviolet irradiation in cultured skin fibroblasts) and genetic testing (mutation in the CSA/ERCC8 or CSB/ERCC6 genes, involved in DNA repair). The disease shows a wide spectrum of presentations and is divided into four clinical subtypes with regard to the age at onset and the severity of the disease. Cerebro-oculo-facio-skeletal syndrome (COFS) is the most severe form, starting in the utero with a rapidly fatal outcome. CS2 begins in the first few years of life and leads to death in infancy. CS1, considered as the classical and the most frequent form, begins in childhood with

a fatal outcome in late childhood. CS3 shows milder clinical signs and follows a more protracted course into adulthood.

Brain imaging plays a crucial role in suggesting the diagnosis of CS. Brain white matter (WM) signal abnormalities on MRI, basal ganglia calcifications on CT and brain atrophy, predominantly in the posterior fossa, are cardinal features of the disease. A previous study described neuroimaging in CS and showed that CS is primarily a hypomyelinating disorder.[1] Striking differences in imaging were also found between the subtypes of the disease. The more severe types (CS2 and COFS) were characterized by early atrophy, severe hypomyelination and calcifications distributed in a particular pattern within the cortex and the subcortical WM as well as within the leptomeningeal vessels. In contrast, atrophy and hypomyelination were lower in the less severe form (CS3). Recently, van der Voorn et al[2] attempted to classify leukodystrophies into different groups using the magnetic transfer ratio (MTR), diffusion tensor imaging (DTI) and MR spectroscopy.[2] Apparent diffusion coefficient (ADC) values were close to normal values in hypomyelination and significantly increased in demyelinating disorders, vacuolating and cystic degeneration ($p < 0.001$). Fractional anisotropy (FA) was slightly but significantly decreased compared with controls in hypomyelinating disorders ($p < 0.01$) and highly decreased in demyelination, myelin vacuolation and cystic degeneration ($p < 0.001$).

Therefore, the aim of this DTI study in CS was first to determine the DTI parameters in CS and to characterize the CS subtypes based on DTI measurements; a volumetric brain analysis was also performed to quantify brain volume loss and to look for differences between subtypes. The second objective was to determine whether DTI findings may correspond to findings observed in patients with hypomyelinating disorders.

METHODS AND MATERIALS

Patients

14 patients with proven CS (13 genetically, 1 biochemically; 8 males, 6 females; age range, 1.5–28 years; mean age, 8.5 years) (Table 1) were enrolled in a prospective study and underwent brain MRI. Sedation with oral chloral hydrate was used when needed. There were two patients with CS3 (15 and 28 years old), seven patients with CS1 (6–16 years), three patients with CS2 (1.5–3 years) and two patients with COFS (2 years). 12 of them were included in a previous study.[1] The control group included age- and sex-matched typically developing subjects who underwent MRI for different reasons, such as headaches and orofacial mass. Brain MRI was retrospectively considered normal in these subjects. The local ethics review committee approved the study, and written informed consent was obtained for all participants or their legal guardians.

Imaging

DTI and volumetric imaging were performed on a 1.5-T MRI scanner (Siemens Avanto, Erlangen, Germany) in patients and controls as part of a complete brain MRI examination that also included sagittal T_1 weighted [repetition time (TR)/echo time (TE)/excitations/acquisition time, 452 ms/9 ms/1/1 min 43 s, axial proton density and T_2 weighted (TR/TE/excitations/acquisition time, 4000 ms/14–109 ms/1/2 min 42 s) and fluid-attenuated inversion-recovery (TR/TE/inversion time/excitations/acquisition time, 9290 ms/116 ms/2500 ms/1/3 min 56 s) images]. Volumetric imaging was obtained from a three-dimensional fast low-angle shot axial T_1 weighted sequence (TR/TE/excitations/acquisition time, 11 ms/4.94 ms/1/5 min 34 s; field of view 25 cm, matrix 224×256 pixels; 176 slices; voxel $1 \times 1 \times 1$ mm, gap 20%). DTI was acquired in the axial plane (TR/TE/flip angle, 6800 ms/99 ms/90°, field of view = 230 mm, matrix = 128×128 pixels, section thickness/intersection gap 3.5 mm/0, number of excitations = 2, resulting in a voxel size of $1.8 \times 1.8 \times 3.5\ mm^3$). Diffusion-sensitizing gradient encoding was applied sequentially in 30 non-collinear directions with 2 b-values ($b = 0$–$700\ s\ mm^{-2}$ <4 years, $b = 0$–$1000\ s\ mm^{-2}$ >4 years); 41 axial slices of 3.5-mm thickness covering the whole brain were acquired in 7.1 min in all patients. In patients who were young with small brains, the uppermost slices were located outside the brain and were not included in post-processing. Criteria for inclusion in the study were defined as an MRI study free of motion artefacts.

Data post-processing

Brain diffusion tensor imaging analysis

10 of the patients had a good-quality DTI sequence and could be analyzed with regions of interest (ROIs), first with whole-brain analysis and then left semiovale centre analysis. The DTI sequence did not include the posterior fossa in two of these patients. The FA, ADC maps and DTI eigenvalues were computed from DT images using the proprietary software of the scanner manufacturer (Neuro3D, Siemens Healthcare, Erlangen, Germany).

Whole-brain analysis The distribution of DTI indices (FA and ADC) (expressed as mean ± standard deviation) was analyzed over different brain ROIs manually defined on the axial b0

Table 1. Patients with Cockayne syndrome (CS): clinical and demographic data

Patients	1	2	3	4	5	6	7	8	9	10	11	12	13	14
Sex	M	F	F	M	F	F	M	M	M	M	M	M	F	F
Age (years)	15	28	6	7	8	7	8	13	16	1	3	3	2	2
Head circumference (SD)	−4	−3.5	−6	−10	−5	−4	−4	−8	−3.5	−8	−7	−8	−8.5	−7.5
CS subtype	3	3	1	1	1	1	1	1	1	2	2	2	COFS	COFS
Genetic mutation	CSB	CSB	CSB	CSA	CSA	CSB	CSA	CSA	CSA	CSB	CSB	CSB	CSB	CSB

COFS, cerebro-oculo-facio-skeletal syndrome; F, female; M, male; SD, standard deviation.

images: centrum semiovale (CSO), frontal WM (FWM), parietal, occipital and temporal WM, corpus callosum (CC) genu and splenium, anterior limb of the internal capsule and posterior limb of the internal capsule (PLIC), cerebral and cerebellar peduncles, pons and cerebellar WM (Figure 1). All ROIs were drawn bilaterally except for the CC and the pons. The size of the circular ROI was adjusted to the volume of the structure studied. ROIs were placed away from calcifications within the WM by referring to the CT scan. The basal ganglia and thalamus were not analyzed because calcifications were frequent in these locations, which could alter the results, particularly ADC values (Figure 2).

Left centrum semiovale analysis In the second step, a single ROI was placed in the left CSO with calculation of the ADC, FA, axial (λ_1) and transverse diffusivity ($\lambda_t = (\lambda_2 + \lambda_3)/2$) first to compare the main diffusion indices (ADC and FA) with the van der Voorn et al[2] study and second to gain insight into the pathogenesis of WM alteration with DTI eigenvalues.

Brain volumetric analysis

All 14 patients were analyzed. Total brain volume and infratentorial volume (ITV) (brainstem and cerebellum) were obtained by applying in-house-implemented segmentation software (Medimax-Medipy, http://piiv.u-strasbg.fr/traitement-images/medipy) with automatic and manual segmentation, performed by the first author. Massive calcifications of the basal ganglia were excluded by the segmentation tool, as the cranial bone, because they were both recognized as bone tissue. However, lighter and cortical calcifications were not distinguished from brain parenchyma by the software. The boundary of the infratentorial area was delineated according to previous publications.[3] The volume of each part of the brain was calculated by quantifying the number of voxels present. ITV was also normalized to total brain volume to estimate ratios.

Figure 1. An example of region of interest placement on an axial *b*0 image in the frontal and parietal white matter.

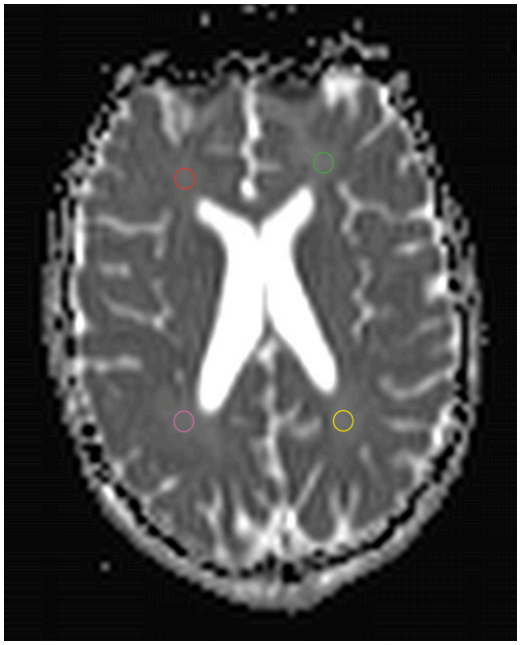

Statistical analysis

Brain diffusion tensor imaging analysis

Whole-brain analysis The DTI parameters of patients with CS and controls were compared for each ROI for FA and ADC using the Student's *t*-test. A *p*-value <0.05 was considered significant.

Two groups were then created to compare the DTI parameters between patients with CS because of the small number of patients within each CS subtype. The moderate group included patients with CS1 and CS3 (six patients) and patients with severe CS2 and COFS (four patients). To examine group differences, the Student's *t*-test was applied for each ROI in each subgroup for FA and ADC. A *p*-value <0.05 was considered significant.

Left centrum semiovale The FA, ADC, λ_1, λ_2, λ_3 and λ_t values of the patients with CS were obtained. After logarithmic transformation, the values were compared with controls using the Student's *t*-test with a *p*-value <0.05 considered significant.

Brain volumetric analysis

After logarithmic transformation, brain volumes were compared between patients with CS and controls and between the CS3 + CS1 and CS2 + COFS groups using the Student's *t*-test.

A *p*-value <0.05 was considered significant.

RESULTS

Brain diffusion tensor imaging analysis

Whole-brain analysis

Comparison between patients with Cockayne syndrome and controls A significantly ($p < 0.05$) decreased FA and increased ADC was found in patients with CS compared with controls within the FWM and temporal WM, CSO, genu and splenium of the CC (Table 2). A significantly increased ($p < 0.05$) ADC was also seen in patients with CS within the internal capsules,

Figure 2. An axial CT scan of a patient with Cockayne syndrome 2 (2 years old) showing bilateral calcifications in the basal ganglia and in the cortex at the depths of the sulci in the frontal and parietal lobes.

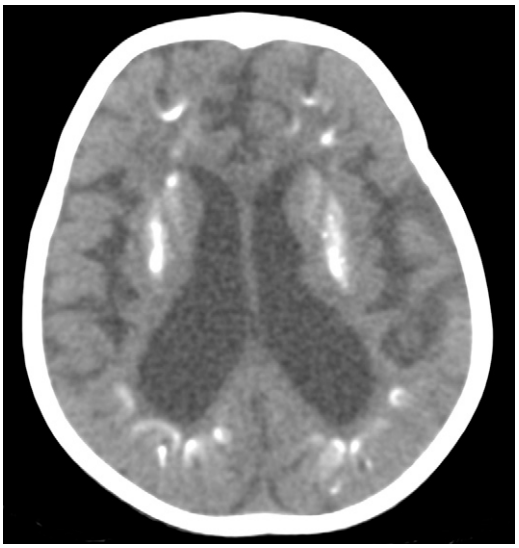

Table 2. Whole-brain diffusion tensor imaging analysis: comparison of the mean fractional anisotropy (FA) and apparent diffusion coefficient (ADC) values between the patients with Cockayne syndrome and control groups

FA	Mean FA values		Mean Differences	*p*-value	ADC	Mean ADC values			*p*-value
	Patients	Controls				Patients	Controls	Mean Differences	
CSO R	245.42 ± 52.16	356.72 ± 69.11	**−111.3**	**0.004711**	**CSO R**	1108.67 ± 42.29	854.16 ± 56.7	**254.51**	**0.0009789**
CSO L	254.7 ± 61.04	353.39 ± 84.89	**−98.69**	**0.02176**	**CSO L**	1124.13 ± 52.47	866.52 ± 65.72	**257.61**	**0.001246**
FWM R	238.44 ± 56.25	335.44 ± 71.92	**−97**	**0.04911**	**FWM R**	1163.5 ± 56.18	926.36 ± 57.39	**237.14**	**0.005556**
FWM L	225.21 ± 44.8	363.21 ± 79.84	**−138**	**0.02408**	**FWM L**	1140.9 ± 65.47	929.11 ± 54.46	**211.79**	**0.002943**
PWM R	257.96 ± 51.57	378.58 ± 83.67	**−135.35**	**0.01452**	PWM R	1060.93 ± 65.96	924.09 ± 57.64	140.34	0.07574
PWM L	246.8 ± 42.37	380.94 ± 83.86	**−139.9**	**0.009021**	PWM L	1104.33 ± 50.84	941.12 ± 70.2	158.07	0.1013
TWM R	290.45 ± 54.89	366.67 ± 57.99	**−76.22**	**0.02023**	**TWM R**	1098.42 ± 58.49	955.72 ± 53.76	**142.7**	**0.02881**
TWM L	308.92 ± 54.67	387.41 ± 55.67	**−78.49**	**0.04555**	**TWM L**	1153.12 ± 51	960.18 ± 59.58	**192.94**	**0.01325**
OWM R	289.07 ± 48.56	460.1 ± 99.45	−169.37	**0.004326**	OWM R	986.5 ± 36.78	875.38 ± 58.21	110.03	0.07793
OWM L	293.95 ± 43.02	428.54 ± 112.18	−119.35	0.05918	OWM L	1004.6 ± 60.41	885.11 ± 61.54	121.92	0.05167
CC genu	609 ± 46.44	851.73 ± 74.67	**−242.73**	**$1.822e^{-05}$**	**CC genu**	1059.61 ± 67.98	801.69 ± 136.59	**257.92**	**0.001388**
CC splenium	568.93 ± 46.03	798.25 ± 57.92	**−221.31**	**0.003405**	**CC splenium**	1125.02 ± 99.28	839.91 ± 89.75	**290.61**	**0.006617**
ICAL R	370.96 ± 102	497.38 ± 128.96	**−155.86**	**0.03852**	**ICAL R**	874.8 ± 68.32	830.84 ± 74.73	**75.36**	**0.004124**
ICAL L	379.46 ± 118.16	472.56 ± 153.56	−121.56	0.06056	**ICAL L**	888.22 ± 65.18	825.87 ± 85.25	**91.5**	**0.03157**
PLIC R	461.38 ± 118.17	553.96 ± 143.85	−86.77	0.054	**PLIC R**	922.8 ± 62.86	807.43 ± 66.22	**112.13**	**$7.50e^{-05}$**
PLIC L	476.9 ± 118.11	621.31 ± 107.77	**−140.11**	**0.004879**	**PLIC L**	934.77 ± 62.12	809.58 ± 66.53	**118.58**	**0.0003313**
Cerebral peduncle R	451.2 ± 77.54	439.03 ± 134.05	12.17	0.7302	Cerebral peduncle R	901.58 ± 61.2	893.72 ± 81.74	7.86	0.7999
Cerebral peduncle L	527.51 ± 68.71	477.23 ± 154.05	50.28	0.3253	Cerebral peduncle L	897.65 ± 81.56	888.73 ± 86.91	8.92	0.819
Pons	273.35 ± 101.3	374.77 ± 129.67	**−102.13**	**0.005745**	Pons	895.57 ± 81.33	850.04 ± 119.91	37.9	0.3121
Cerebellar peduncle R	572.23 ± 71.5	659.62 ± 92.24	−67.76	0.09704	**Cerebellar peduncle R**	850.42 ± 51.55	756.43 ± 62.42	**83.83**	**0.01303**
Cerebellar peduncle L	526.93 ± 79.33	629.77 ± 105.63	−96.48	0.05628	**Cerebellar peduncle L**	878.41 ± 63.12	768.73 ± 72.09	**110.03**	**0.003847**
Cerebellar WM R	341.41 ± 62.38	342.88 ± 83.11	10.27	0.7613	**Cerebellar WM R**	892.97 ± 45.42	776.31 ± 63.55	**92.57**	**0.003089**
Cerebellar WM L	338.02 ± 59.77	328.9 ± 75.94	3.24	0.9229	**Cerebellar WM L**	895.5 ± 49.04	779.37 ± 62.2	**93.6**	**0.0165**

CC, corpus callosum; CSO, centrum semiovale; FWM, frontal white matter; ICAL, anterior limb of the internal capsule; L, left; OWM, occipital white matter; PLIC, posterior limb of the internal capsule; PWM: parietal white matter; R, right; TWM, temporal white matter; WM, white matter.
Values are expressed as mean ± standard deviation. FA values ($\times 10^{-3}$); ADC values ($\times 10^{-6}\,mm^2\,s^{-1}$); a *p* value <0.05 was considered significant.

Figure 3. (a) An axial apparent diffusion coefficient map of a patient with Cockayne syndrome 1 (9 years old) showing high signal intensity in the bilateral centrum semiovale (CSO). (b) Corresponding axial T_2 weighted MR image is demonstrating bilateral mild hyperintensity in CSO suggesting hypomyelination.

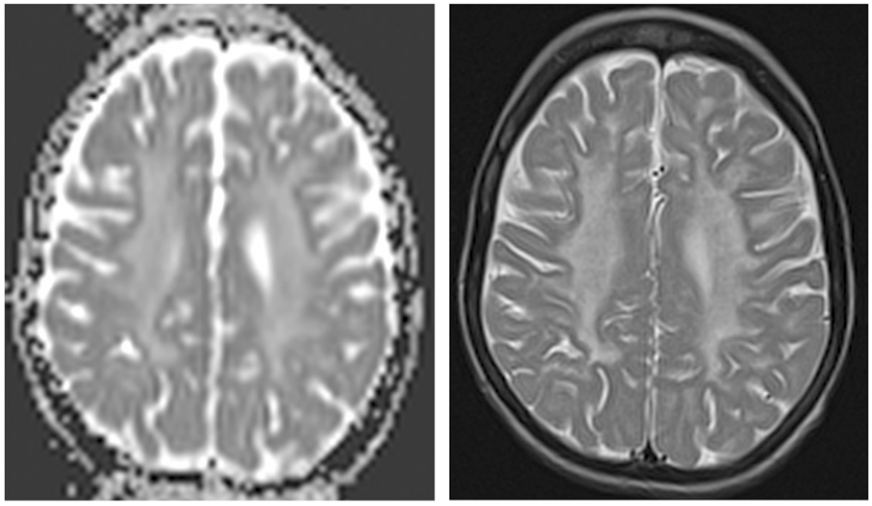

cerebellar peduncles and cerebellar hemispheres. The greatest ADC differences between patients and controls were found in the CC and CSO (Figure 3).

Comparison between groups of patients with Cockayne syndrome Statistical analysis revealed significant and non-significant group differences in DTI indices (Table 3). Higher ADC values were observed in most of the WM in the most severe CS subgroup; but, only the ADC values in the splenium of the CC and PLIC were significantly higher ($p < 0.05$). Comparison of the FA values showed more heterogeneous results, but only the FA in the cerebral peduncles was significantly lower ($p < 0.05$) in the more severe group compared with that in the less severe group of severity.

Left centrum semiovale analysis

A significantly decreased FA and increased ADC was found in patients with CS compared with controls within the left CSO (Table 4). The ADC was increased in CS by 38.18%, with a mean ADC value of $1179.2 \times 10^{-6}\,mm^2\,s^{-1}$ ($\pm$ 139.86), close to the hypomyelination group in the study of van der Voorn et al [$1070 \times 10^{-6}\,mm^2\,s^{-1}$ ($\pm$180)]. The FA was 58% lower in CS, with a mean FA value of 0.204 ± 0.04, closer to the demyelination (0.18 ± 0.04) than the hypomyelination (0.28 ± 0.05) group in the study of van der Voorn et al.[2] Both λ_t (+51%) and λ_1 (+12%) diffusivity values were increased.

Considering DTI parameter values with increasing age, absolute ADC values were steady, while FA values were lower, and all three eigenvalues and λ_t were higher.

Brain volumetric analysis

Total brain volume was significantly reduced in patients with CS compared with that in controls by $57.06 \pm 9.5\%$ (mean $\pm$ standard deviation) (Table 5). The brain volume reduction was greater in the posterior fossa ($68.68 \pm 11.9\%$) than in the supratentorial area ($55.3 \pm 9.7\%$), with an ITV normalized by total brain volume in patients with CS ($8.9 \pm 1.9\%$) significantly lower than that in controls ($12.5 \pm 1\%$).

Total brain volume loss was significantly higher in the severe type of CS (CS2 and COFS) ($65.8 \pm 6.3\%$) than in the moderate type (CS3 and CS1) ($52.2 \pm 9.1\%$) (Figure 4). No statistical differences were observed for infratentorial brain volume normalized by total brain volume between the CS2/COFS ($8.70 \pm 1.57\%$; mean age, 2 years) and CS1/CS3 subgroups ($9.09 \pm 2.16\%$; mean age, 9 years).

DISCUSSION

This study compared the DTI metrics and brain volume of patients with CS and controls. Significant differences were observed between CS and controls and between CS subtypes. DTI metrics showed lower FA values and higher ADC values in most WM structures in patients with CS. The ADC and eigenvalues were consistent with hypomyelination. Brain volume loss reached 50% and was predominant within the posterior fossa.

Diffusion tensor imaging analysis

Hypomyelinating disorders are the largest subgroup of leukodystrophies of unknown origin.[4] Like other hypomyelinating diseases, CS manifests as an aspecific, diffuse, moderate high signal intensity of the supratentorial WM on T_2 weighted imaging, with intermediate or slight high signal intensity on T_1 weighted imaging.[5,6] Additional imaging findings may help in the diagnosis of CS, such as basal ganglia calcifications and brain atrophy predominant in the posterior fossa, but the diagnosis remains difficult if these are lacking. Moreover, the prognosis differs widely between the different CS subtypes, which may be difficult to discriminate clinically because of overlapping features.[7] Conventional imaging with T_1 weighted imaging and T_2 weighted imaging helps discriminate CS subtypes.[1] However,

Table 3. Diffusion tensor imaging analysis of the whole brain: comparison between Cockayne syndrome (CS) subtypes

ROI	Mean FA value		Mean differences	*p*-value	ROI	Mean ADC value		Mean differences	*p*-value
	CS1 + CS3	CS2 + COFS				CS1 + CS3	CS2 + COFS		
CSO R	227 ± 47.73	273.05 ± 58.80	−46.05	0.3583	CSO R	1125.93 ± 47.04	1082.77 ± 35.17	43.16	0.5842
CSO L	244.60 ± 43.73	269.85 ± 87	−25.25	0.5415	CSO L	1130.38 ± 48.6	1114.75 ± 58.27	15.63	0.8458
FWM R	206.01 ± 49.25	287.07 ± 66.75	−81.06	0.2117	FWM R	1163.98 ± 71.66	1162.77 ± 32.95	1.21	0.9924
FWM L	177.16 ± 35.36	297.27 ± 58.95	−120.11	0.1863	FWM L	1135.31 ± 67.5	1149.27 ± 62.42	−13.96	0.9074
PWM R	253.44 ± 49.28	263.62 ± 54.45	−10.18	0.8072	PWM R	1094.62 ± 76.14	1018.82 ± 53.25	75.8	0.4629
PWM L	230.18 ± 42.88	267.57 ± 41.75	−37.39	0.5279	PWM L	1171.34 ± 65.7	1020.57 ± 32.27	150.77	0.2029
TWM R	309.25 ± 57.38	262.25 ± 51.15	47	0.3282	TWM R	1053.55 ± 60.06	1165.72 ± 56.12	−112.17	0.3184
TWM L	309.36 ± 48.80	308.25 ± 63.47	1.11	0.9868	TWM L	1102.51 ± 64.63	1229.02 ± 30.55	−126.51	0.329
OWM R	288.9 ± 54.02	289.3 ± 41.75	−0.4	0.991	OWM R	997.78 ± 46.02	972.40 ± 25.25	25.38	0.8054
OWM L	272 ± 50.96	321.4 ± 33.10	−49.4	0.1473	OWM L	1020.12 ± 44.26	985.20 ± 80.60	34.92	0.6612
Genu CC	629.35 ± 54.78	578.47 ± 33.92	50.94	0.3621	Genu CC	978.4 ± 75.38	1181.42 ± 56.87	−203.02	0.158
Splenium CC	638.76 ± 52.72	452.56 ± 34.90	186.2	0.08103	**Splenium CC**	973.04 ± 80.24	1378.33 ± 131.03	−405.29	**0.008057**
ICAL R	N/A	N/A			ICAL R	N/A	N/A		
ICAL L	N/A	N/A			ICAL L	N/A	N/A		
PLIC R	469.06 ± 139.18	451.80 ± 91.92	17.26	0.7643	**PLIC R**	873.1 ± 72.76	984.92 ± 50.5	−111.82	**0.03274**
PLIC L	527.16 ± 130.84	414.07 ± 102.20	113.09	0.1601	**PLIC L**	895.82 ± 61.98	983.47 ± 62.30	−87.65	**0.0448**
Cerebral peduncle R	494.95 ± 100.68	385.57 ± 42.82	109.38	**0.02318**	Cerebral peduncle R	886.8 ± 70.63	923.75 ± 47.05	−36.95	0.5643
Cerebral peduncle L	572.53 ± 76.55	459.97 ± 56.95	112.56	**0.04723**	Cerebral peduncle L	852.15 ± 77.2	965.9 ± 88.1	−113.75	0.1295
Pons	263.97 ± 110.6	282.72 ± 92	−18.75	0.5272	Pons	853.52 ± 99.25	937.62 ± 63.42	−84.1	0.2057
Cerebellar peduncle R	603.57 ± 85.7	540.9 ± 57.3	62.67	0.343	Cerebellar peduncle R	825.42 ± 43.3	875.42 ± 59.8	−50	0.2329
Cerebellar peduncle L	546.6 ± 88.65	507.27 ± 70.02	44.33	0.5866	Cerebellar peduncle L	839.25 ± 64.8	917.57 ± 61.45	−78.32	0.1849
Cerebellar WM R	374.96 ± 72.5	316.25 ± 54.8	58.76	0.3448	Cerebellar WM R	836.26 ± 59.53	935.5 ± 34.85	−99.24	0.07379
Cerebellar WM L	334.9 ± 57.7	340.37 ± 61.32	−5.47	0.93	Cerebellar WM L	858.76 ± 45.86	923.05 ± 51.42	−64.29	0.1608

ADC, apparent diffusion coefficient; CC, corpus callosum; COFS, cerebro-oculo-facio-skeletal syndrome; CSO, centrum semiovale; FA, fractional anisotropy; FWM, frontal white matter; ICAL, anterior limb of the internal capsule; L, left; N/A, not available; OWM, occipital white matter; PLIC, posterior limb of the internal capsule; PWM: parietal white matter; R, right; ROI, region of interest; TWM, temporal white matter; WM, white matter.
Values are expressed as mean ± standard deviation. FA values ($\times 10^{-3}$); ADC values ($\times 10^{-6}$ $mm^2 s^{-1}$); *p*-value <0.05 was considered significant.

Table 4. Diffusion tensor imaging analyses on the left centrum semiovale: comparison between patients with Cockayne syndrome (CS) and controls

DTI parameter	Group of patients with CS	Control group	*p*-value
FA	204 ± 40	351 ± 50	$p < 0.001$ Percentage decrease FA: 58%
ADC	1179.2 ± 139.86	853.38 ± 93.50	$p < 0.001$ Percentage increase ADC: 38%
λ_1	1432.76 ± 149.63	1167.48 ± 83.23	$p < 0.001$ Percentage increase λ_1: 12%
λ_2	1144.78 ± 160.56	832.34 ± 132.27	$p < 0.001$ Percentage increase λ_2: 37%
λ_3	960.27 ± 138.63	560.34 ± 94.83	$p < 0.001$ Percentage increase λ_3: 71%
λ_t	1052.53 ± 144.77	696.34 ± 103.11	$p < 0.001$ Percentage increase λ_t: 51%

ADC, apparent diffusion coefficient; FA, fractional anisotropy.
Values are expressed as mean ± standard deviation. FA values ($\times 10^{-3}$); ADC, λ_1, λ_2, λ_3, λ_t values ($\times 10^{-6}\,mm^2\,s^{-1}$). *p*-value <0.05 was considered significant.

other imaging techniques enabling a quantified evaluation of CS severity would be clinically helpful, in particular in evaluating therapeutic interventions more precisely.

DTI can better detect, characterize and discriminate WM diseases than standard MRI sequences by measuring the microscopic diffusion of water molecules. ADC reflects water diffusivity, and myelin is only one of the factors that influence ADC. The other factors include axonal cellular membranes, dendrites and synapses, glial cells and free water. The increase in ADC values is due to increased extracellular space, which may be related to tissue matrix damage, as in the case of cystic and spongiform degeneration,[2] decreased cellularity, increased and/or hypertrophic glial cells[8] and vasogenic oedema. High and steady ADC values are observed in diseases with hypomyelination such as Pelizaeus–Merzbacher disease; the ADC values in this clinical condition correspond to the normal values of developing WM observed from birth to 6 months.[9,10]

A previous study combining quantitative parameters from MR spectroscopy, MTR and DTI[2] showed that ADC was not statistically different from controls in the hypomyelinating group of patients, but showed a statistically significant increase in creatine ($p < 0.5$) and myo-Inositol ($p < 0.001$) and a decrease in MTR ($p < 0.001$) and FA ($p < 0.01$). The present study showed statistically significant differences for both ADC and FA values obtained within the CSO ($p < 0.001$) between patients with CS and controls, with an increased mean ADC value in patients with CS ($1179.2 \times 10^{-6}\,mm^2\,s^{-1}$ ±139.86). The statistically significant differences in ADC values in our study may be explained by the lower mean ADC values in controls in the present study compared with the study of van der Voorn et al, possibly related to the fact that controls and patients were strictly age and sex matched. The mean ADC value in patients with CS is close to the hypomyelination category reported by van der Voorn et al[2] and to the values observed during normal brain development in 6-month-old infants[11] and 2- to 4-month-old infants.[12] This suggests that CS is a hypomyelinating

Table 5. Comparison of brain volumes between patients with Cockayne syndrome (CS) and controls (left), and between CS subtypes (right)

Brain volume	CS patients	Controls	*p*-value	CS2 + COFS	CS1 + CS3	*p*-value
WBV (mm^3)	501324.86 ± 144376	1154959.7 ± 132345.36	$p < 0.001$ Percentage WBV reduction: 57.06 ± 9.54%	353792.2 ± 144376.42	583287.44 ± 116385.8	$p < 0.001$ Percentage WBV reduction relative to corresponding controls: CS1 + CS3: 52.4 ± 7% CS2 + COFS: 65.2 ± 9%
ITV (mm^3)	45366.43 ± 19.222.98	144049.42 ± 15126.48	$p = 2905e^{-11}$ Percentage PFV reduction: 68.68 ± 11.9%	31020 ± 19223	53336 ± 18920	$p = 0.00876$
STV (mm^3)	455958.43 ± 128324.65	1010910.3 ± 120963.38	$p = 1.436e^{-11}$ Percentage STV reduction: 52.2 ± 9.1%	322772 ± 153112.86	529950.89 ± 102618.7	$p = 0.0002417$
ITV/WBV	8.9 ± 1.9%	12.6 ± 0.9%	$p < 0.001$	9.1 ± 2.2%	8.7 ± 1.7%	$p = 0.7$

COFS, cerebro-oculo-facio-skeletal syndrome; ITV, infratentorial volume; STV, supratentorial volume; WBV, whole-brain volume.
Values are expressed as mean ± standard deviation. *p* value <0.05 was considered significant.

Figure 4. Comparison between three-dimensional volume rendering MR reconstructions of the brain of a 2-year-old patient with Cockayne syndrome (CS) 2 (a), a 16-year-old patient with CS1 (b) and a 15-year-old patient with CS3 (c).

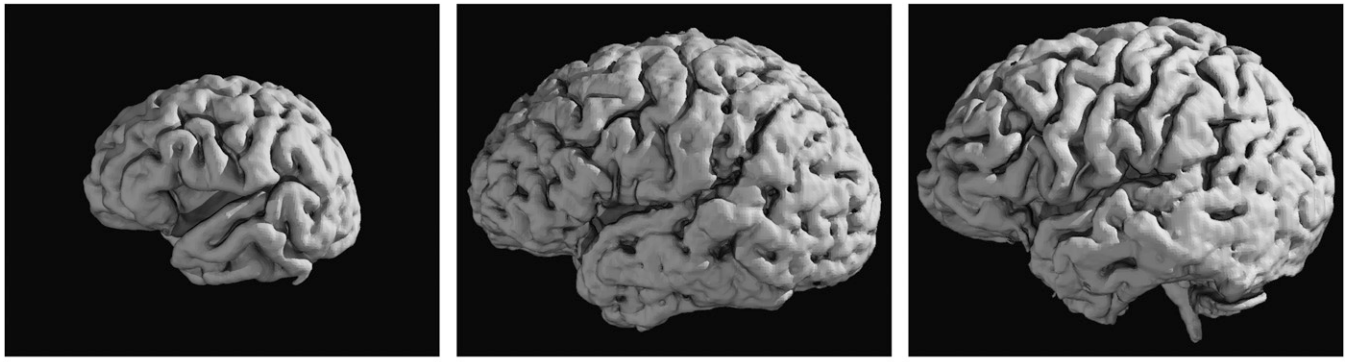

disorder. However, secondary destruction of myelin may also contribute to high ADC values in CS, although ADC would be higher and associated with a low T_1 signal intensity. Multimodal MRI including DTI, the recently developed myelin water fraction mapping technique and MTR may better assess myelination in CS.[13]

Although longitudinal MRI follow-up was not available, ADC values found in the CSO were stable with increasing age. Conversely, FA values in the CSO decreased with increasing age, and mean FA values were close to demyelinating disorders.[2] These findings could be explained by the progressive atrophy observed over time in CS. In the hypomyelination category in the study of van der Voorn et al, FA was only slightly decreased, contrary to the demyelinating category, and atrophy was not reported as a significant finding. Indeed, the main source of WM anisotropy is not myelin integrity, but much more axonal cellular membrane integrity and fibre density/compaction/alignment,[14] which are affected in both demyelinating disorders and atrophy. However, the comparison of our data with those of van der Voorn et al is limited, as the technical parameters and processing of DTI were not strictly the same.

DTI metrics showed lower FA values ($p < 0.05$) and higher ADC values ($p < 0.05$) in most brain structures in patients with CS, even in those unaffected by signal abnormalities such as cerebellar peduncles. The greatest ADC differences between patients and controls were found in the CC, CSO and FWM, while the greatest FA differences were observed in the CC, parietal and FWM and CSO. This correlated well with conventional MRI as those areas showed high T_2 signal intensities in patients with CS. DTI was even more sensitive by detecting abnormalities not apparent on conventional MRI in the cerebellum and pons.

In terms of severity, DTI metrics showed statistically significant differences (higher ADC, lower FA values) ($p < 0.05$) in severe cases compared with moderate cases within the CC splenium and PLIC (ADC), and in the cerebral peduncles (FA). This is concordant with the different signal intensities observed on conventional MRI in the different subtypes in these structures. Indeed, a high T_2 signal intensity was observed within central WM tracts (internal capsule and CC) in the more severe CS groups in a previous study,[1] indicating absent myelination, while a low signal intensity was present in the less severe group, indicating myelination. Moreover, DTI showed FA differences in the cerebral peduncles that were not detected by conventional MRI. The differences found between CS subtypes should be interpreted with caution owing to the small number of patients, but this demonstrates that DTI provides an objective and quantitative imaging marker of severity in CS and is slightly more sensitive regarding CS subtype distinction than conventional MRI. Even if DTI seems slightly more sensitive than conventional MRI to detect WM abnormalities in patients with CS and between CS subtypes, the additional information is not really relevant. Also, the patients included in this study were very young, so prolonged MRI examinations with DTI are not desirable. One of the potential advantages of DTI in CS may be monitoring of therapeutic intervention closely.

Two directional parameters can be extracted from DTI: axial diffusivity and radial or transverse diffusivity.[15] Animal models and DTI/post-mortem histology correlations have demonstrated that these parameters are non-invasive markers of axons (integrity/compaction) and myelin sheaths (demyelination/remyelination), respectively.[16] In our study, axial and moreover radial diffusivity values were significantly increased in the CSO ($p < 0.001$). These DTI parameter modifications in CS were close to those observed in a mouse model of Pelizaeus–Merzbacher disease,[8] which were attributed to astrocyte hypertrophy (reactional gliosis) and myelin defects, respectively. Striking similar neuropathological findings were observed in CS, consisting of diffuse cerebral and cerebellar WM atrophy with a discontinuous multifocal myelination defect and fibrillary gliosis in myelin-defective zones.[17,18]

The pathophysiology of myelin abnormalities in CS is ascribed to both neurodevelopmental failure and neurodegeneration. Initially, a transcriptional defect leads to a low amount of myelin produced by oligodendrocytes, which could explain the hypomyelination observed on imaging. The small amount of myelin may be of poor quality and spontaneously broken down progressively or by defective maintenance by oligodendrocytes that disappear owing to apoptosis related to an accumulation of DNA errors.[19] This could explain the progressive atrophy/shrinkage

of the WM observed on imaging, as in all end-stage leukodystrophies.[20]

Brain volumetric analysis

Overall, we found significant brain atrophy/volume reduction in patients with CS compared with healthy controls ($p < 0.001$). This was closely correlated with the profound microcephaly usually observed in all patients beyond 2 years of age. Our mean value of 57 ± 9.4% brain volume reduction concurs with pathological studies, reporting >50% brain atrophy, mainly in the WM.[21,22] Brain atrophy was greater in patients with CS2 and COFS than that in patients with CS3 and CS1 ($p < 0.001$). This is also in accordance with neuropathological reports and with the more severe microcephaly observed in CS2 and COFS.[18,23]

Predominant atrophy/volume reduction in the posterior fossa confirms previous pathological CS studies.[24] Clinically, it correlates with the cerebellar syndrome observed consistently in patients with CS.[7] Prominent cerebellar atrophy could be explained by combined atrophy/volume reduction of the cerebellar cortex and WM, while WM atrophy is predominant in the supratentorial area.[17,22,25] The pathophysiological background of selective vulnerability of the cerebellar cortex may be based on ongoing neuronal proliferation, particularly for granule cells in the external granular layer, during the first year of life, which explains postnatal cerebellar enlargement.[26] Atrophy is a non-specific finding that occurs at the end-stage of many leukodystrophies. However, progressive severe atrophy, predominantly in the posterior fossa, is observed in few leukodystrophies apart from CS and is a common sign of DNA repair diseases such as CS, xeroderma pigmentosum and ataxia-telangiectasia.[27]

We did not find statistically significant differences between the two severity groups, COFS/CS2 and CS1/CS3, concerning the degree of the infratentorial brain volume atrophy/volume reduction relative to total cerebral volume. This may indicate that the pathophysiological mechanism of volume reduction applies equally to the infratentorial and supratentorial areas in both groups.

Limitations of the study

The main limitations of this study are the small number of patients with analyzable data owing to the rarity of CS, the wide age distribution and the cross-sectional design of the study; these factors limit the conclusions drawn from this study. We used a 1.5-T MR scan. Higher field strength[28] and multishell diffusion imaging[29] could provide more accurate and specific data about pathological WM structure. Another technical limitation of the study lies in the different b-values used for patients under 4 years of age ($b = 700\ s\ mm^{-2}$) and after 4 years of age ($b = 1000\ s\ mm^{-2}$), limiting the comparisons between the groups, knowing the b-value dependence of DTI parameters quantification.[30] Concerning DTI data analysis, we used ROI analysis, but a voxel or tract-based statistical analysis could have provided more robust and informative data on specific tract systems. However, those techniques could not be used because of the differences in brain size and major WM atrophy of patients with CS.[31]

The reproducibility of the brain volume measurements depends on the software segmentation tool used, imaging hardware and acquisition parameters, making comparisons between studies difficult. However, given the relatively high volumetric differences observed between patients with CS and controls, minimal differences would be observed between software programs. A complementary longitudinal study evaluating more patients would provide additional information on the temporal dynamics of DTI parameters as well as brain volume loss in CS.

CONCLUSION

Our findings demonstrate that DTI-derived metrics and volumetric analysis provide quantitative information for the characterization of CS. Compared with conventional MRI, DTI is slightly more sensitive for the detection of WM abnormalities in CS and in the distinction of CS subtypes. Even if DTI does not seem essential for the diagnosis and distinction of CS subtypes, these complementary quantitative data may be particularly useful for monitoring therapeutic intervention.

REFERENCES

1. Koob M, Laugel V, Durand M, Fothergill H, Dalloz C, Sauvanaud F, et al. Neuroimaging in Cockayne syndrome. *AJNR Am J Neuroradiol* 2010; **31**: 1623–30. doi: http://dx.doi.org/10.3174/ajnr.A2135
2. van der Voorn JP, Pouwels PJ, Hart AA, Serrarens J, Willemsen MA, Kremer HP, et al. Childhood white matter disorders: quantitative MR imaging and spectroscopy. *Radiology* 2006; **241**: 510–17. doi: http://dx.doi.org/10.1148/radiol.2412051345
3. Luft AR, Skalej M, Schulz JB, Welte D, Kolb R, Burk K, et al. Patterns of age-related shrinkage in cerebellum and brainstem observed *in vivo* using three-dimensional MRI volumetry. *Cereb Cortex* 1999; **9**: 712–21. doi: http://dx.doi.org/10.1093/cercor/9.7.712
4. van der Knaap MS, Breiter SN, Naidu S, Hart AA, Valk J. Defining and categorizing leukoencephalopathies of unknown origin: MR imaging approach. *Radiology* 1999; **213**: 121–33. doi: http://dx.doi.org/10.1148/radiology.213.1.r99se01121
5. Rossi A, Biancheri R, Zara F, Bruno C, Uziel G, van der Knaap MS, et al. Hypomyelination and congenital cataract: neuroimaging features of a novel inherited white matter disorder. *AJNR Am J Neuroradiol* 2008; **29**: 301–5. doi: http://dx.doi.org/10.3174/ajnr.A0792
6. Steenweg ME, Vanderver A, Blaser S, Bizzi A, de Koning TJ, Mancini GM, et al. Magnetic resonance imaging pattern recognition in hypomyelinating disorders. *Brain* 2010; **133**: 2971–82. doi: http://dx.doi.org/10.1093/brain/awq257
7. Laugel V. Cockayne syndrome: the expanding clinical and mutational spectrum. *Mech Ageing Dev* 2013; **134**: 161–70. doi: http://dx.doi.org/10.1016/j.mad.2013.02.006
8. Harsan LA, Poulet P, Guignard B, Parizel N, Skoff RP, Ghandour MS. Astrocytic hypertrophy in dysmyelination influences the

diffusion anisotropy of white matter. *J Neurosci Res* 2007; **85**: 935–44. doi: http://dx.doi.org/10.1002/jnr.21201

9. Sener RN. Pelizaeus-Merzbacher disease: diffusion MR imaging and proton MR spectroscopy findings. *J Neuroradiol* 2004; **31**: 138–41. doi: http://dx.doi.org/10.1016/S0150-9861(04)96980-5
10. Engelbrecht V, Scherer A, Rassek M, Witsack HJ, Modder U. Diffusion-weighted MR imaging in the brain in children: findings in the normal brain and in the brain with white matter diseases. *Radiology* 2002; **222**: 410–18. doi: http://dx.doi.org/10.1148/radiol.2222010492
11. Provenzale JM, Liang L, DeLong D, White LE. Diffusion tensor imaging assessment of brain white matter maturation during the first postnatal year. *AJR Am J Roentgenol* 2007; **189**: 476–86. doi: http://dx.doi.org/10.2214/AJR.07.2132
12. Schneider JF, Il'yasov KA, Hennig J, Martin E. Fast quantitative diffusion-tensor imaging of cerebral white matter from the neonatal period to adolescence. *Neuroradiology* 2004; **46**: 258–66. doi: http://dx.doi.org/10.1007/s00234-003-1154-2
13. Barkovich AJ, Deon S. Reprint of hypomyelinating disorders: an MRI approach. *Neurobiol Dis* 2016; **92**: 46–54. doi: http://dx.doi.org/10.1016/j.nbd.2015.10.022
14. Beaulieu C. The basis of anisotropic water diffusion in the nervous system—a technical review. *NMR Biomed* 2002; **15**: 435–55. doi: http://dx.doi.org/10.1002/nbm.782
15. Song SK, Sun SW, Ramsbottom MJ, Chang C, Russell J, Cross AH. Dysmyelination revealed through MRI as increased radial (but unchanged axial) diffusion of water. *Neuroimage* 2002; **17**: 1429–36. doi: http://dx.doi.org/10.1006/nimg.2002.1267
16. Harsan LA, Poulet P, Guignard B, Steibel J, Parizel N, de Sousa PL, et al. Brain dysmyelination and recovery assessment by noninvasive *in vivo* diffusion tensor magnetic resonance imaging. *J Neurosci Res* 2006; **83**: 392–402. doi: http://dx.doi.org/10.1002/jnr.20742
17. van der Knaap MS, Valk J. Magnetic resonance of myelination and myelin disorders. In: *Magnetic resonance of myelination and myelin disorders*. 3rd edn. Berlin, Germany: Springer; 2005. pp. 259–67.
18. Patton MA, Giannelli F, Francis AJ, Baraitser M, Harding B, Williams AJ. Early onset Cockayne's syndrome: case reports with neuropathological and fibroblast studies. *J Med Genet* 1989; **26**: 154–9. doi: http://dx.doi.org/10.1136/jmg.26.3.154
19. Weidenheim KM, Dickson DW, Rapin I. Neuropathology of Cockayne syndrome: evidence for impaired development, premature aging, and neurodegeneration. *Mech Ageing Dev* 2009; **130**: 619–36. doi: http://dx.doi.org/10.1016/j.mad.2009.07.006
20. Patay Z. Diffusion-weighted MR imaging in leukodystrophies. *Eur Radiol* 2005; **15**: 2284–303. doi: http://dx.doi.org/10.1007/s00330-005-2846-2
21. Rapin I, Weidenheim K, Lindenbaum Y, Rosenbaum P, Merchant SN, Krishna S, et al. Cockayne syndrome in adults: review with clinical and pathologic study of a new case. *J Child Neurol* 2006; **21**: 991–1006. doi: http://dx.doi.org/10.1177/08830738060210110101
22. Leech RW, Brumback RA, Miller RH, Otsuka F, Tarone RE, Robbins JH. Cockayne syndrome: clinicopathologic and tissue culture studies of affected siblings. *J Neuropathol Exp Neurol* 1985; **44**: 507–19. doi: http://dx.doi.org/10.1097/00005072-198509000-00006
23. Del Bigio MR, Greenberg CR, Rorke LB, Schnur R, McDonald-McGinn DM, Zackai EH. Neuropathological findings in eight children with cerebro-oculo-facio-skeletal (COFS) syndrome. *J Neuropathol Exp Neurol* 1997; **56**: 1147–57. doi: http://dx.doi.org/10.1097/00005072-199710000-00009
24. Caviness VS Jr, Kennedy DN, Richelme C, Rademacher J, Filipek PA. The human brain age 7–11 years: a volumetric analysis based on magnetic resonance images. *Cereb Cortex* 1996; **6**: 726–36. doi: http://dx.doi.org/10.1093/cercor/6.5.726
25. Itoh M, Hayashi M, Shioda K, Minagawa M, Isa F, Tamagawa K, et al. Neurodegeneration in hereditary nucleotide repair disorders. *Brain Dev* 1999; **21**: 326–33.
26. Knickmeyer RC, Gouttard S, Kang C, Evans D, Wilber K, Smith JK, et al. A structural MRI study of human brain development from birth to 2 years. *J Neurosci* 2008; **28**: 12176–82. doi: http://dx.doi.org/10.1523/JNEUROSCI.3479-08.2008
27. Brooks PJ, Cheng TF, Cooper L. Do all of the neurologic diseases in patients with DNA repair gene mutations result from the accumulation of DNA damage? *DNA Repair (Amst)* 2008; **7**: 834–48. doi: http://dx.doi.org/10.1016/j.dnarep.2008.01.017
28. Alexander AL, Lee JE, Wu YC, Field AS. Comparison of diffusion tensor imaging measurements at 3.0 T *versus* 1.5 T with and without parallel imaging. *Neuroimaging Clin N Am* 2006; **16**: 299–309. doi: http://dx.doi.org/10.1016/j.nic.2006.02.006
29. Timmers I, Zhang H, Bastiani M, Jansma BM, Roebroeck A, Rubio-Gozalbo ME. White matter microstructure pathology in classic galactosemia revealed by neurite orientation dispersion and density imaging. *J Inherit Metab Dis* 2015; **38**: 295–304. doi: http://dx.doi.org/10.1007/s10545-014-9780-x
30. Hui ES, Cheung MM, Chan KC, Wu EX. B-value dependence of DTI quantitation and sensitivity in detecting neural tissue changes. *Neuroimage* 2010; **49**: 2366–74. doi: http://dx.doi.org/10.1016/j.neuroimage.2009.10.022
31. Mukherjee P, Chung SW, Berman JI, Hess CP, Henry RG. Diffusion tensor MR imaging and fiber tractography: technical considerations. *AJNR Am J Neuroradiol* 2008; **29**: 843–52. doi: http://dx.doi.org/10.3174/ajnr.A1052